Mat. Res. Soc. Symp. Proc. Vol. 674 © 2001 Materials Research Society

# Magnetic Properties of Self-Assembled Fe Nanoparticle Arrays

D. Farrell, S. Yamamuro, and S. A. Majetich
Dept. of Physics, Carnegie Mellon University
Pittsburgh, PA 15213, U.S.A.

## ABSTRACT

The magnetic properties of multilayer arrays of Fe nanoparticles were compared with those of frozen, dilute suspensions of the same particles. The array sample displayed larger coercivity in both hysteretic and remanent magnetization measurements. However, the derivative of the remanent magnetization curve shows a much broader switching field distribution for the arrays than for the dilute sample. Magnetic relaxation measurements show the convergence of the time dependent properties of the samples at large times, and much more rapid relaxation in the arrays at short times.

## INTRODUCTION

Dipolar interactions have long been known to affect the switching fields of nanoparticles [1]. However, with a large distribution of interparticle distances, these effects have been difficult to quantify. Improved synthetic methods have made it possible to prepare monodisperse magnetic nanoparticles that self-assemble into arrays [2, 3]. Here we reexamine the effect of dipolar interactions in these nanoparticle arrays, which lend themselves to numerical computation of the dipolar fields.

In this paper we present experimental results showing how the switching fields of the arrays differ from those of a dilute sample made from the same nanoparticles. The magnetic properties are measured at low temperatures so that the particles do not move. At room temperature these particles are superparamagnetic, but at low temperature hysteresis is observed.

## EXPERIMENTAL

Monodisperse Fe nanoparticles were prepared under an argon atmosphere. 4 mg of platinum acetylacetonate was dissolved in 15 mL of octyl ether in the presence of 150 mg of the reducing agent 1,2-hexadecanediol. The solution was then warmed to 100 °C and 0.2 mL of $Fe(CO)_5$ was added. The heating continued until the solution reached 280 °C, at which point the heating mantle was removed and the solution was heated again to 260 °C. While heating the platinum salt is reduced to form platinum clusters, onto which iron atoms from the thermally decomposed $Fe(CO)_5$ preferentially deposit. The solution was cooled, and an additional 15 mL of octyl ether was added. At 100 °C 1.5 mL of $Fe(CO)_5$ was added, and the heating continued to 260 °C. The amount of iron added determines the final size of the particles; for these experiments, the average particle size was 8 nm. However, the large arrays were formed preferentially from particles 6 nm in

diameter; larger particles were confined to the edges of the arrays. The fluid was kept under an inert atmosphere, and 0.025 mL each of the surfactants oleylamine and oleic acid were added to the cooled solution. Ethanol was added to precipitate the iron particles, and after decanting the supernatant the particles were redispersed in hexane. The concentration of surfactant in the solvent was kept constant throughout the washing procedure.

The structural properties of the resulting particles were characterized by transmission electron microscopy (TEM). Here a TEM grid was dipped into the solution and suspended in an argon atmosphere to dry. The grids were then imaged in a Philips EM420 electron microscope (120 kV accelerating voltage) to reveal the particle array structures.

For magnetic characterization, two types of sample were prepared. Dilute suspensions of the particles were prepared by diluting the ferrofluid to one-tenth the original concentration. The estimated final concentration was 0.8 mg/mL (0.01% volume, assuming a density of 7.86 g/mL). The dilute fluid was placed into a glass ampoule, which was sealed under argon. The array sample consisted of ten stacked, particle-coated TEM grids. TEM screening verified the presence of arrays and uniformity of coating over the grids. The plane of the grids was *perpendicular* to the field direction within the Quantum Design MPMS2 SQUID magnetometer.

The samples were magnetically characterized by regular and remanent hysteresis loops, and by magnetic relaxation measurements. All measurements were performed at 10 K. For the hysteresis loops, the field was applied and the magnetic moment of the sample was measured; after each at-field measurement, the field was applied and turned off, and the remanent moment $M_r$ was measured. The at-field measurements form the regular hysteresis loop, and the zero field measurements form the remanent hysteresis loop. In magnetic viscosity or relaxation measurements, the sample was first saturated at 50 kOe. The field was then reduced to zero, or a reverse field equal to the coercivity $H_c$ was applied. The moment of the sample was measured at 90 – 600 sec time intervals over a ten hour period at this field. For the array sample it was necessary to correct for the large diamagnetic signal arising from the carbon coated copper TEM grids. The diamagnetic contribution was estimated by calculating the slope of the straight line data acquired at fields above 35 kOe. This contribution was subtracted prior to data analysis.

## RESULTS AND DISCUSSION

We assume that the samples were identical except for the effect of magnetic dipolar interactions between particles. For the array sample, the center-to-center particle spacing was approximately 9 nm as measured by TEM [4]. The sample consisted of mainly hexagonally close packed structural domains of Fe nanoparticles, typically ~100 nm across and several layers thick. For the dilute sample, the average particle spacing estimated from the mass concentration was greater than 500 nm.

Comparison of regular and remanent magnetization loops show higher coercivities for the arrays (760 Oe) than the dilute sample (300 Oe). However, these measurements include rotational effects, which are absent from the remanent

magnetization curves shown in Figure 1. Here, $H_c$ was 2760 Oe for the arrays and 550 Oe for the dilute sample.

The increased $H_c$ in the arrays sample suggests that the dipolar interactions stabilize the particles against magnetization reversal. The fringe fields of the surrounding particles create a local field $\mathbf{H}_{loc}$, and the effective field $\mathbf{H}_{eff} = \mathbf{H}_{loc} + \mathbf{H}_{applied}$. Magnetically isolated, uniaxial monodomain particles with their easy axes parallel to $\mathbf{H}_{applied}$ will all switch at the same field $\mathbf{H}_{sw}$ [5]. This leads to a perfectly square hysteresis loop with a delta function switching field distribution.

We can see how the larger coercivity arises from dipolar interactions. Assume that a particle switches its magnetization direction when $\mathbf{H}_{eff} = \mathbf{H}_{sw}$, and that $\mathbf{H}_{eff}$ depends on the distribution of the surrounding particle moments. At saturation the particle moments are aligned with the applied field, perpendicular to the plane of the TEM grid, as shown in Figure 2a. The fringe field of one particle causes a destabilizing local field at its neighbors, but $\mathbf{H}_{loc}$ is small compared with $\mathbf{H}_{applied}$. As soon as the field is removed, the particle moments begin to reorient. In the absence of an external field the lowest energy configuration for a two-dimensional lattice will have the magnetic moments in the plane of the lattice [6]. Within the plane the dipolar interactions favor the formation of chains of particles, and neighboring chains have opposite moment directions, as shown in Figure 2b. Once chains have formed the local field will be in-plane. Near neighbor calculations estimate this field to be on the order of 2500 Oe. Only when the applied field is larger than this do the particle moments switch to lie perpendicular to the TEM grid. The arrays studied here have multiple layers and finite structural domains, so their behavior will be somewhat more complex than that shown in Figure 2. However, there is clearly rapid relaxation of the magnetization associated with dipolar interactions in the arrays.

The switching field distribution was found from the derivative of the remanent hysteresis loop, $dM_r/dH$, as shown in Figure 3. The dilute sample $dM_r/dH$ curve is broadened with respect to a delta function. The breadth could arise from several sources. Our particles are not uniaxial and they have randomly oriented easy axes. Some particles in the dilute sample may be closely associated, though the average spacing is large. The

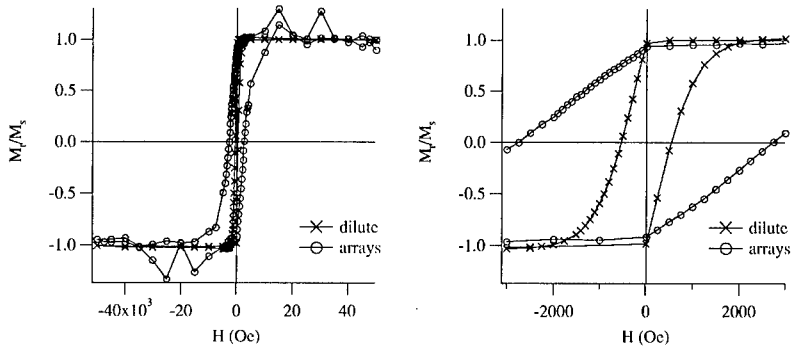


**Fig. 1.** Remanent magnetization loops taken for dilute and arrays samples of 6 nm Fe nanoparticles at 10 K. The magnetizations are normalized to the saturation values.

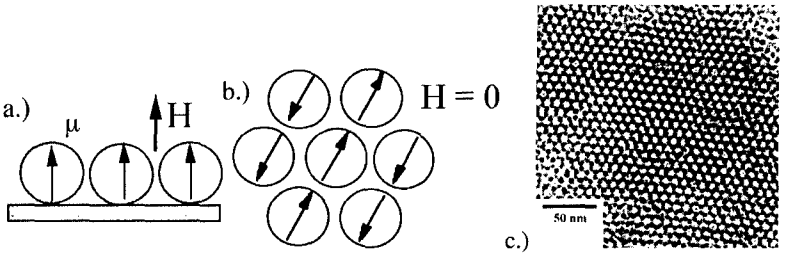


**Fig. 2.** a.) Nearest neighbor moments at saturation, with the field normal to the plane of the TEM grid. b.) Equilibrium orientation of nearest neighbor moments in zero field. c.) TEM image of Fe multilayer, showing hexagonal symmetry. Dark spots represent phase contrast of overlapping particles; light spots are regions with less particle overlap.

arrays have an even broader switching field distribution, indicating a broader distribution of energy barriers than in the dilute sample. Variation of the local field over the area of the sample leads to a range of local fields, and therefore switching occurs over a range of applied fields. Even though the arrays have a larger coercivity, they contain many particles with low barriers to switching of the magnetization direction.

For the arrays, the switching field distribution will depend not only on the distribution of easy axis orientations, but also on the uniformity of particle environments and array orientations with respect to the field. A distribution of switching fields will arise from the distribution of hexagonal array orientations. In addition, the local field will be very different for particles near grain boundaries than for those located within a domain. Greater structural uniformity of the arrays should narrow the switching field distribution, as should crystallographic alignment of the particles.

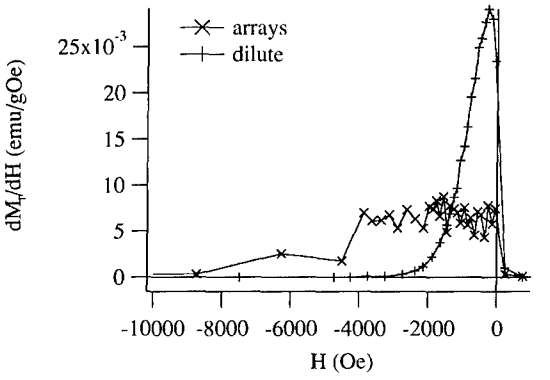


**Fig. 3.** Switching field distributions for dilute and arrays samples of Fe.

A second way to characterize the distribution of energy barriers is through magnetic relaxation measurements (Figure 4). This distribution causes the magnetization to decay logarithmically in time, so that $M = M_0 - S\ln(t/t_0)$ [7, 8]. Here, $M_o$ is the initial magnetization at field, S is the slope of the line, and $t_o$ is the time of the initial measurement. By different choices of the initial time $t_0$ the value of the magnetization intercept $M_0$ is changed, but the value of the slope S is not.

Figure 4 shows the magnetic relaxation of the arrays and the dilute sample both at zero field and at the coercivity of the regular hysteresis loop. The dilute samples show logarithmic decay at all times, but the arrays have a dramatic drop in the magnetization at early times, followed by logarithmic decay. Figure 5 illustrates the magnetic viscosity S found from the slope of the plots of Figure 4. S is larger at the coercivity than at zero field, as expected [9]. The larger relaxation rate in the arrays seems at first to be inconsistent with the greater coercivity, relative to the dilute sample. We postulate that the rapid initial relaxation arises due to chain formation like that in Figure 2b. Once the chains have formed, the dipolar local fields prevent further switching until much greater

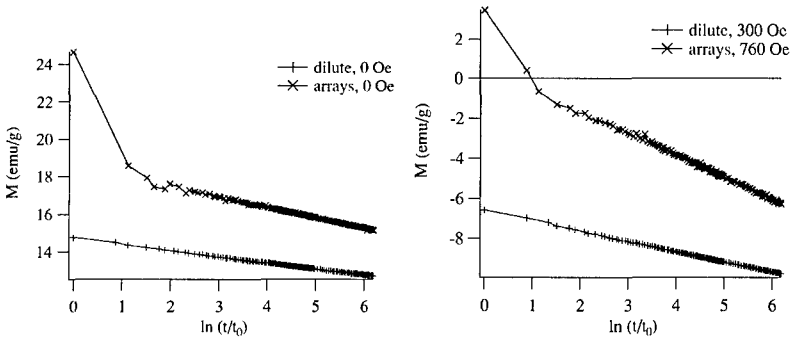


**Fig. 4.** M vs. ln ($t/t_0$) at 10 K. Left: H = 0; Right: arrays, H = 760 Oe; dilute, H = 300 Oe.

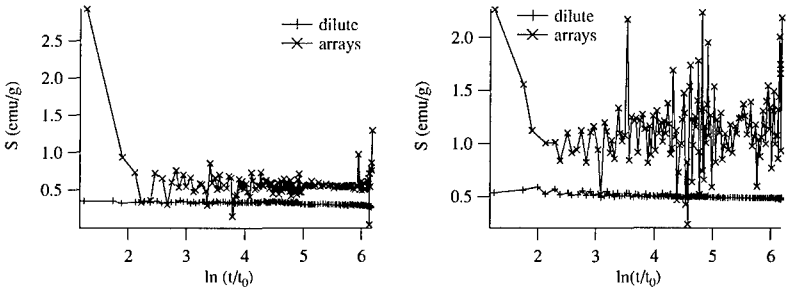


**Fig. 5.** S versus ln ($t/t_0$). Left: H = 0; Right: arrays, H = 760 Oe; dilute, H = 300 Oe.

fields are applied. Because the particles are not crystallographically oriented when the arrays are self-assembled, there is a broad range of switching fields for chain formation. The long time behavior may be dominated in both samples by the distribution of energy barriers associated with variations in the easy axis orientations of the particles [10].

## CONCLUSIONS

The results of magnetic measurements on samples of Fe nanoparticles in frozen, dilute suspensions and ordered in hcp arrays indicates the effect of a local field arising from dipole interactions between Fe particles. Based on simulations of TEM images, the particles studied here had 6 nm cores and a spacing of 3 nm between the surfaces of the iron cores. The self-assembled iron nanoparticle arrays have a larger coercivity than a dilute sample of the same nanoparticles. The enhanced coercivity can be understood qualitatively in terms of the average local field due to dipolar interactions with neighboring particles. The arrays also have a much broader distribution of switching fields than the dilute sample. Magnetic relaxation measurements show comparable relaxation rates for the arrays and dilute samples at long times, but much more rapid relaxation in the arrays over a short time period. This is attributed to the rapid formation of chains of dipoles following the application of a reverse field.

## ACKNOWLEDGMENTS

We would like to acknowledge support from the National Science Foundation grant #CTS-9800127 and the American Chemical Society Petroleum Research Fund grant #ACS PRF 33866-AC5.

## REFERENCES

1. B. D. Cullity, *Introduction to Magnetic Materials* (Addison-Wesley, Reading, MA, 1972), p. 387.
2. S. Sun. C. B. Murray, D. Weller, L. Folks, and A. Moser, Science **287**, 1989 (2000).
3. C. Petit, A. Taleb, and M. P. Pileni, *J. Phys. Chem.* **103**, 1805 (1999).
4. S. Yamamuro, D. Farrell, S. A. Majetich, MRS Symposium Proceedings, Fall 2000, paper D10.8.
5. E. C. Stoner, F. R. S. and E. P. Wohlfarth, Phil. Trans. Roy. Soc. **240**, 599 (1948).
6. G. Mukhopadhyay, P. Apell, and M. Hanson, J. Magn. Magn. Mater. 203, 286 (1999).
7. R. Street and J. C. Woolley, Proc. Phys. Soc. *A* **62**, 562 (1949).
8. R. W. Chantrell, M. Fearon, and E. P. Wohlfarth, Phys. Stat. Sol. (a) **9** , 213 (1986).
9. S. A. Majetich and E. M. Kirkpatrick, IEEE Trans. Mag. **33**, 3721 (1997).
10. K. D. Humfeld, A. K. Giri, S. A. Majetich, and E. L. Venturini, IEEE Trans. Mag. (in press, 2001).